Amine Modification of Calcium Phosphates by Low-Pressure CH4/N2/He Plasma for Bone Regeneration

Joe Kodama
Department of Orthopaedic Surgery, Osaka University Graduate School of Medicine
Anjar Anggraini Harumningtyas
Center for Atomic and Molecular Technologies, Graduate School of Engineering, Osaka University
Tomoko Ito
Center for Atomic and Molecular Technologies, Graduate School of Engineering, Osaka University
Miroslav Michlíček
Plasma Technologies, CEITEC – Central European Institute of Technology, Masaryk University
Satoshi Sugimoto
Center for Atomic and Molecular Technologies, Graduate School of Engineering, Osaka University
Yuichiro Ukon
Department of Orthopaedic Surgery, Osaka University Graduate School of Medicine
Junichi Kushioka
Department of Orthopaedic Surgery, Osaka University Graduate School of Medicine
Rintaro Okada
Department of Orthopaedic Surgery, Osaka University Graduate School of Medicine
Takashi Kamatani
Department of Orthopaedic Surgery, Osaka University Graduate School of Medicine
Kunihiko Hashimoto
Department of Orthopaedic Surgery, Osaka University Graduate School of Medicine
Daisuke Tateiwa
Department of Orthopaedic Surgery, Osaka University Graduate School of Medicine
Hiroyuki Tsukazaki
Department of Orthopaedic Surgery, Osaka University Graduate School of Medicine
Shinichi Nakagawa
Department of Orthopaedic Surgery, Osaka University Graduate School of Medicine
Shota Takenaka
Department of Orthopaedic Surgery, Osaka University Graduate School of Medicine
Takahiro Makino
Department of Orthopaedic Surgery, Osaka University Graduate School of Medicine
Yusuke Sakai

Department of Orthopaedic Surgery, Osaka University Graduate School of Medicine
David Nečas
Plasma Technologies, CEITEC – Central European Institute of Technology, Masaryk University
Lenka Zajíčková
Plasma Technologies, CEITEC – Central European Institute of Technology, Masaryk University
Satoshi Hamaguchi
Center for Atomic and Molecular Technologies, Graduate School of Engineering, Osaka University
Takashi Kaito (takashikaito@ort.med.osaka-u.ac.jp)
Department of Orthopaedic Surgery, Osaka University Graduate School of Medicine

---

Research Article

Keywords: Calcium phosphates, osteogenic, bone

Posted Date: April 8th, 2021

DOI: https://doi.org/10.21203/rs.3.rs-385329/v1

Title:

Amine modification of calcium phosphates by low-pressure $CH_4/N_2/He$ plasma for bone regeneration

Joe Kodama[1,‡], Anjar Anggraini Harumningtyas[2,3,‡], Tomoko Ito[2], Miroslav Michlíček[4,5], Satoshi Sugimoto[2], Yuichiro Ukon[1], Junichi Kushioka[1], Rintaro Okada[1], Takashi Kamatani[1], Kunihiko Hashimoto[1], Daisuke Tateiwa[1], Hiroyuki Tsukazaki[1], Shinichi Nakagawa[1], Shota Takenaka[1], Takahiro Makino[1], Yusuke Sakai[1], David Nečas[4], Lenka Zajíčková[4,5], Satoshi Hamaguchi[2,*], Takashi Kaito[1,*]

[1] Department of Orthopaedic Surgery, Osaka University Graduate School of Medicine, Osaka, 565-0871, Japan

[2] Center for Atomic and Molecular Technologies, Graduate School of Engineering, Osaka University, 2-1 Yamadaoka, Suita, Osaka 565-0871 Japan

[3] Center for Accelerator Science and Technology, National Nuclear Energy Agency of Indonesia (BATAN), Jalan Babarsari Kotak Pos 6101 ykbb Yogyakarta 55281, Indonesia

[4] Plasma Technologies, CEITEC – Central European Institute of Technology, Masaryk University, Kamenice 5, Brno 62500, Czech Republic

[5] Department of Physical Electronics, Faculty of Science, Masaryk University, Kotlářská 2, Brno 61137, Czech Republic

‡ These authors contributed equally to this work

*Corresponding authors

Takashi Kaito, MD, PhD.

Department of Orthopaedic Surgery, Osaka University Graduate School of Medicine, 2-2 Yamadaoka, Suita, Osaka 565-0871, Japan.

Tel: +81-6-6879-3552

Fax: +81-6-6879-3559

E-mail: takashikaito@ort.med.osaka-u.ac.jp

Satoshi Hamaguchi, PhD.

Center for Atomic and Molecular Technologies (CAMT),

Graduate School of Engineering, Osaka University,

2-1 Yamadaoka, Suita, Osaka 565-0871, Japan.

TEL: +81-6-6879-7913 (06-6879-7913)

FAX: +81-6-6879-7916 (06-6879-7916)

E-mail: hamaguch@ppl.eng.osaka-u.ac.jp

Abstract

Calcium phosphates are promising materials for artificial bone but lack of satisfied osteogenic ability on their surfaces. In the present study, we applied a low-pressure plasma technology to chemically (amine) modify the surface of calcium phosphates (hydroxyapatite or beta-tricalcium phosphate) using a CH_4/N_2/He plasm gas mixture to improve their osteogenic ability. The CH_4/N_2/He plasma treatment produced a thin, stable amine-rich carbon polymer on the surface of the calcium phosphates, and enhanced hydrophilicity, deep infiltration of cells into porous calcium phosphates, cell adhesion and osteogenic differentiation on the surface of calcium phosphates. In a rat calvarial defect model, the CH_4/N_2/He plasma treatment afforded calcium phosphates a significant higher bone regeneration capacity. Together, these results suggest that surface modification of calcium phosphates with CH_4/N_2/He plasma might improve osteogenic ability of calcium phosphates in vitro and in vivo.

Introduction

Autogenous iliac bone grafting remains the gold standard for repairing large bone defects caused by trauma or tumors and spinal fusion surgeries. However, the amount of autograft that can be harvested is limited and the harvesting procedure can cause donor site morbidity [1]. To overcome these limitations, the use of artificial bones, in combination with autograft is prevalent. However, the widespread use of artificial bone is hampered by its lack of satisfied osteogenic ability, despite their superiority in terms of bone conduction and availability [2].

Calcium phosphates are representative materials for artificial bone. To enhance the osteogenic ability of calcium phosphates, surface modification mediated by plasma technology has gained considerable attention. Functional groups created by plasma polymerization (i.e., polymer formation via plasma discharges) can provide selected surface properties such as hydrophilicity/hydrophobicity, cytocompatibility, and bacterial resistance to meet different clinical needs [3]. We previously reported that plasma treatment of hydroxyapatite (HA, a typical calcium phosphate used for artificial bone) with O_2/He gas could improve surface hydrophilicity and promote the osteogenic differentiation of rat bone marrow stromal cells (BMSCs). However, the O_2/He plasma-treated HA exerted only minimal effects *in vivo*, possibly owing to the instability of the generated hydroxyl (–OH) groups [4-5]. In the present study, we focused on the addition of amino groups or amines ($–NH_x$ with x = 0–2) to the surface of HA and beta-tricalcium phosphate (β-TCP, another typical calcium phosphate used for artificial bone), which has been suggested to promote cell attachment [6-7]. Using a mixture gas of CH_4/N_2/He as the precursor, we

successfully generated a thin, stable amine-rich carbon polymer on and inside the surfaces of the HA and β-TCP through a low-pressure plasma treatment, and enhanced cell infiltration, migration, cell adhesion, osteogenic differentiation in vitro, and bone regeneration with a rat calvarial defect model *in vivo*.

Materials and methods

Materials and reagents

Both dense disks and porous disks of HA [$Ca_{10}(PO_4)_6(OH)_2$] and β-TCP [$Ca_3(PO_4)_2$] were kindly provided by Coors Tek KK (Tokyo, Japan). Porous disks of both HA and β-TCP had well-organized interconnected structure [8], and contained interconnected pores (porosity; 72–78%, average pore diameter; 150 μm, average diameter of interconnected passages; 40 μm).

The following culture media were used for *in vitro* experiments: (1) growth medium (GM) comprising α Eagle's minimal essential medium (α-MEM, Gibco, ThermoFisher Scientific, Waltham, MA, USA) supplemented with 10% fetal bovine serum (Sigma-Aldrich, St. Louis, MO, USA) and 1% antibiotic-antimycotic solution (Sigma-Aldrich); (2) osteogenic differentiation medium (ODM) consisting of GM supplemented with 50 μg/ml L-ascorbic acid 2-phosphate (Sigma-Aldrich), 10 mM β-glycerol phosphate (Merck KGaA, Frankfurt, Germany), and 10 nM dexamethasone (Sigma-Aldrich).

Cell Counting Kit-8 (CCK-8, Dojindo Molecular Technologies, Kumamoto, Japan) was used for the cell proliferation assay. LabAssay ALP (FUJIFILM Wako Pure Chemical Corporation) was used for the evaluation of alkaline phosphatase (ALP) activity and BCIP/NBT Color Development Substrate (Promega Corp.,

Madison, WI, USA) was used for ALP staining. M-PER and Pierce Rapid Gold BCA Protein Assay Kits (Thermo Fisher Scientific) were used for total protein extraction and quantification, respectively. K-CX AT solution (Falma Co., Tokyo, Japan) was used for decalcification of *in vivo* specimens.

Plasma polymerization of HA and β-TCP disks

Plasma polymerization using a bipolar pulsed-plasma deposition system (also known as an inverter plasma system) was as shown in Fig. 1A. The details of the system are described elsewhere [9-10]. Briefly, HA and β-TCP disks were placed on the bottom metal (molybdenum) electrode, 190 mm in diameter, connected to the bipolar high-voltage power supply. The applied bipolar pulse voltages were 1.3 and - 1.1 kV (peak-to-peak voltage of 2.4 kV) and the pulse duration was 1 μs for each positive or negative pulse. The power, repetition frequency, and duty cycle were 15 W, 5 kHz, and 1%, respectively, such that the time elapse between a positive pulse and the subsequent negative pulse was 100 μs. The upper metal (aluminum) electrode, 80 mm in diameter, was grounded and the distance between the two electrodes was 38 mm. For plasma polymer deposition, the discharge was generated in a CH_4/N_2/He gas mixture with flow rates of 10, 20, and 10 sccm, respectively, at 70 Pa.

Dense disks were treated on single side for 30 min, which were used for *in vitro* experiments; porous disks of HA was treated on single side for 30 min, which were used for cross section analysis; porous disks of β-TCP were treated on both sides for 60 min (30 min for each side), which were used for in vivo experiments.

Plasma polymer film characterization

X-ray photoelectron spectroscopy (XPS) was carried out to determine the chemical compositions of the surfaces of dense disks using the Shimadzu ESCA-850 with a non-monochromatized Mg-K_α (1253.6 eV) X-ray source at Osaka University, Japan. The pass energy was 75 eV and the spot diameter was 8 mm (90% uniformity).

A high-resolution XPS Axis Supra (Kratos Analytical, Manchester, UK) spectrometer at the Central European Institute of Technology (CEITEC), Brno, Czech Republic was used to analyze chemical compositions of plasma polymers, especially those on the inner surfaces of interconnected pores of plasma-treated porous disks. This high-resolution XPS uses an X-ray source of monochromatic Al-K_α 1486.6 eV with an emission current of 15 mA. The spectra were acquired with a pass energy of 20 eV. The analysis area provided by the larger slot aperture was approximately 700 × 300 μm^2.

For cross section analysis, the single side treated porous disk were cut in half at the center and the cross sections were scanned using high-resolution XPS. The measurements were performed on 21 spots with a diameter of 110 µm that were separated by an equal distance of 100 µm along the center axis of the cross-section (Fig. 1B). During the analysis, the pressure of the XPS chamber was maintained at < 10^{-7} Pa. The peaks of XPS signals used for the analyses in this study were C 1s, Ca 2p, N 1s, O 1s, and P 2p.

Detection of primary amines (–NH_2) on CH_4/N_2/He plasma-treated disk surfaces was performed using the standard derivatization with 4-trifluoromethyl-

benzaldehyde (TFBA) [11]. The derivatization reactions of TFBA vapors with the CH_4/N_2/He plasma-treated disk surfaces were allowed to occur in an Ar atmosphere (Ar flow rate of 60 sccm at atmospheric pressure) at room temperature (approximately 25 °C) for 4 h inside the glove box. Relative concentrations of primary amines on the surfaces of the HA and β-TCP were analyzed with ESCA-850 XPS following the derivatization reactions.

To examine the stability of the deposited plasma polymers, we stored CH_4/N_2/He plasma-treated disks in a sterilized dish at room temperature (approximately 24 °C), and then examined relative concentrations of nitrogen and primary amines on the disk surfaces were using ESCA-850 XPS at several time points over 65 days.

Scanning electron microscopy (SEM)

The surfaces of untreated and plasma treated porous HA disks (φ 5 mm × h 2 mm) were observed with a scanning electron microscope (S-4800, Hitachi, Ltd., Tokyo, Japan).

Ethic declarations

All animal work was approved by the Animal Experimentation Committee of our institution (01-070-000) and restrictedly followed ARRIVE guidelines and the National Institutes of Health Guide for the Care and Use of Laboratory Animals [12].

Cells

Rat BMSCs were obtained from the bone shafts of the femora of four 3-week-old green fluorescent protein (GFP)-transgenic male Sprague-Dawley rats (SD-Tg (CAG-EGFP) rat, Japan SLC, Hamamatsu, Japan). Following sacrifice using CO_2 inhalation, both ends of the femur were removed from the epiphysis; the marrow was flushed out using 10 ml of GM expelled from a syringe through a 21-gauge needle according to the previously described method [13]. The released cells were collected in two 100 mm culture dishes containing 15 ml of GM. The medium was changed after 24 h to remove hematopoietic cells and renewed twice weekly. Cultures were maintained in a humidified atmosphere of 95% air with 5% CO_2 at 37 °C. When the cells reached 80–90% confluency they were washed with phosphate-buffered saline (PBS) and trypsinized with 1% trypsin-ethylenediaminetetraacetic acid (EDTA). Following centrifugation for 5 min at 400 g, the cells were resuspended and plated at a density of $3.6 \times 10^4/cm^2$. After again reaching confluency, cells were collected and stored at -80 °C (Passage 1). Prior to *in vitro* experiments, stocked cells were thawed and resuspended in 15 ml of GM, then plated in a 100 mm dish and cultured for three days to reach 80-90% confluency (Passage 2).

Morphology analysis of adhered cells

Cell suspension (5×10^3 cells/35 µl GM) was gently dropped on dense β-TCP disks (φ 5 mm × h 2 mm) and incubated for 3 h in a 24-well culture plate to initiate adhesion. Then, wells were slowly filled with 1 ml of GM and incubation was continued for another 24 h. Macro fluorescence photos of random areas were obtained. The open source software CellProfiler (www.cellprofiler.org) [14] was

used for sorting cells and cell morphology analysis. In particular, the cell area was measured to quantify the spreading of attached BMSCs. Two cell-shape descriptors (circularity and solidity) were investigated; circularity indicates the closeness of the cell shape to a perfect circle, and solidity is an index to quantify the amount and size of concavities of the cell [15]:

$$Circularity = \frac{4\pi A}{P^2}$$

where *A* is the cell area and *P* is the perimeter.

$$Solidity = \frac{A}{ConvexA}$$

where *ConvexA* is the area of the smallest convex hull that contains the cell.

Cell adhesion assay

Cell suspensions (5 x 10^3 cells/35 µl GM) were gently dropped on dense β-TCP disks (φ 5 mm x h 2 mm) to form centroclinal water drops on the disks. After incubating for 30 min, a centrifugation cell adhesion assay was performed [16]. Briefly, 1 ml of PBS was gently added into the wells and fluorescent macro-photos were obtained to quantify the initial adherent cells. β-TCP disks on which cells were attached were then embedded into a 48-well culture plate containing 100 µl of Vaselin. After filling each well with PBS, the plate was sealed with sealing tape. Then, the culture plate was set upside-down on a centrifuge and centrifuged at 10 *g* for 5 min to detach weakly adherent cells. PBS and detached cells were slowly aspirated, then the wells were carefully filled with 200 µl PBS. Macro fluorescence photos were obtained using the same conditions as prior to the centrifugation. Automatic cell counting was performed using ImageJ software [17].

The adhesion rate was calculated as follows:

$$Adhesion\ \ Rate = \frac{Cell\ \ Number_{before\ \ centrifugation}}{Cell\ \ Number_{after\ \ centrifugation}} \cdot 100\ \ \%$$

Cell proliferation assay

To balance the initial cell count of adherent cells on plasma-treated and untreated β-TCP disks, two different concentrations (5 × 10^3 cells/35 µl GM for the untreated group and 3 × 10^3 cells/35 µl GM for the plasma-treated group) of cell suspension were dropped on dense β-TCP disks (φ 5 mm x h 2 mm) in a 48-well plate. After incubating for 30 min, 500 µl of GM was slowly added into each well. At day 1, 3, 5, 7, 11, and 14, 50 µl of CCK-8 solution was added to each well and the plate was incubated for 2 h, then 100 µl of GM from each well was transferred into a 96-well plate. Optical density at 450 nm was measured using a spectrophotometer (Multiskan GO, Thermo Fisher Scientific).

Osteogenic differentiation assay

A total of 2 × 10^4 cells/35 µl GM were dropped on dense β-TCP disks (φ 5 mm × h 2 mm) for 30 min in a 48-well plate to initiate adhesion. Then, 500 µl of GM was slowly added into the wells, incubated for 24 h, and the culture medium substituted with ODM for osteogenic differentiation. The subculture was maintained for another four days. After washing the disks twice with PBS, the attached cells were fixed using 500 µl of 4% PFA for ALP staining according to the manufacturer's instructions. For ALP activity, 60 µl of M-PER was added to each well and the cells were detached from the disks using a mini scraper. After lysing the cells for 5 min, supernatant was collected for ALP and total protein

assays. An ALP activity unit was defined as the release of 1 nmol p-nitrophenol per min of incubation at 37 °C for one β-TCP disk. The total protein content of the samples was measured to standardize the ALP activity values.

Rat calvarial defect model

A total of 20, 8-week-old male Sprague-Dawley rats (Charles River Laboratories Japan, Yokohama, Japan) were used to generate the calvarial defect model. Anesthesia was maintained by intraperitoneal injection of a mixture of 0.15 mg/kg medetomidine, 2.0 mg/kg midazolam, and 2.5 mg/kg butorphanol after introducing anesthesia by inhalation of 5% isoflurane. A 1.5 cm longitudinal incision was made at the center of the vertex and two full-thickness bone defects with a diameter of 5 mm were then carefully created using a high-speed trephine burr under constant irrigation with saline to avoid heat injury of the surrounding tissue. The CH_4/N_2/He plasma-treated and untreated β-TCP disks were implanted in the right and left defects, respectively. The rats were given free access to water and food. Rats were sacrificed at 3 (n = 5) and 6 (n = 15) weeks by CO_2 inhalation. Microfocus computed tomography (micro-CT) and histological analyses were performed to evaluate new bone formation in the inner pores of β-TCP disks at 3 and 6 weeks.

Microfocus computed tomography (micro-CT)

Harvested specimens were fixed in 10% buffered formalin, dehydrated and degreased using a graded ethanol series, and stored in 70% ethanol at 4 °C for micro-CT scanning (Skyscan 1272 micro-CT , Bruker, Kontich, Belgium) with the

following parameters: Camera binning = 2x2, Source voltage (kV) = 80, Source current (µA) = 125, Image pixel size (µm) = 4, Rotation step (degree) = 0.6, Filter = Al 1 mm. Image analysis was performed using CTAN software (Version 1.18.8.0+, Brucker). The micro-CT images corresponding to the histological sections were compared and the intensities of the newly formed bone and the residual β-TCP were determined and the respective areas extracted (Fig. 1C).

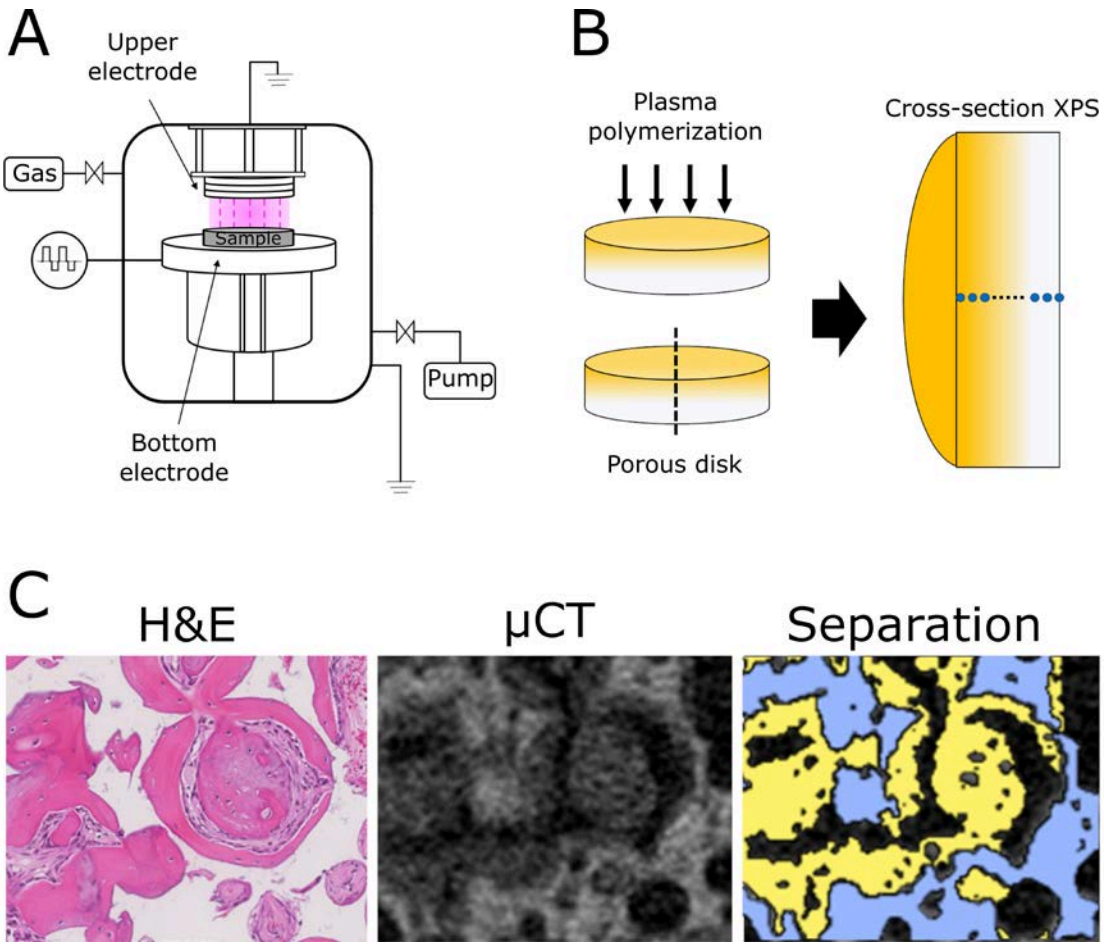

Figure 1. Plasma generation system, methodology of cross-section XPS analysis and micro CT evaluation. (A) Schematic diagram of the pulsed-plasma deposition system used in this study. Samples were placed on the bottom electrode. The discharge chamber was filled with a gas mixture of CH_4, N_2, and He at 70 Pa and bipolar high-

voltage short pulses were applied to the bottom electrode periodically to generate the plasma. (B) Schematic diagram of cross-section XPS analysis. A porous disk was treated with the plasma on a single side and cut in half to expose the cross section. Then, the chemical compositions along the center axis were measured. (C) H&E-stained histological sections and corresponding micro-CT slices were compared to identify β-TCP (blue area) and newly formed bone (yellow area). Unstained areas in histological sections constitute the areas containing remaining β-TCP, which were decalcified. Pink areas stained by eosin reflect newly formed bone inside the β-TCP, which correspond to the gray areas in micro-CT slices. An original algorithm was designed to extract and calculate the volume of β-TCP and newly formed bone separately.

Histological evaluation

After micro-CT scanning, specimens were demineralized using K-CX AT solution at 4 °C, cleared in xylene, and embedded in paraffin. Then, sections of 4 μm thickness were created from the center of specimens and stained with hematoxylin and eosin (H&E).

Statistical analysis

Statistical analysis was performed using GraphPad Prism version 7.04 for Windows (GraphPad Software, San Diego, CA, USA) applying the Mann–Whitney U test for non-parametric data, student's t-test for parametric data, and Wilcoxon matched-pairs signed rank test for *in vivo* results. The values are presented as mean ± standard deviation (SD). The differences were considered

statistically significant for p value < 0.05.

Results

Plasma polymerization on calcium phosphate porous disks

The atomic percentages of calcium (Ca), phosphorus (P), oxygen (O), and carbon (C) was 27.5 ± 0.8, 13.9 ± 0.5, 46.4 ± 0.4, and 12.2 ± 1.2 at.% on the surface of the untreated porous HA, and 28.5 ± 0.2, 14.0 ± 1.5, 44.0 ± 0.6, and 13.4 ± 2.2 at.% on the surface of the untreated dense β-TCP, respectively. After excluding C, the atomic percentages were Ca:P:O = 31.3:15.8:52.8 for the porous HA surface and 32.9:16.2:50.9 for the dense β-TCP surface, which exhibited a Ca-rich stoichiometry compared with the theoretically ideal HA (Ca:P:O = 25.0:10.0:65.0), and β-TCP (Ca:P:O = 23.1:15.4:61.5).

The atomic percentages of Ca, P, O, C, and N, on the surfaces of CH_4/N_2/He plasma-treated porous HA disks was 0.0 ± 0.0, 0.0 ± 0.0, 8.2 ± 3.6, 78.1 ± 3.5, and 13.6 ± 1.9 at.%. A separate measurement performed using a Si substrate exposed to the same CH_4/N_2/He plasma revealed that the deposited plasma polymer film thickness was approximately 100 nm, which is consistent with our XPS measurements.

Fig. 2A shows the change in atomic percentage of N atoms in the polymer film on porous HA disks from the day of polymerization (day 0) to day 65. It was observed that percentage of N atoms in the deposited polymer film remained in the range of 12–15 at.%.

Fig. 2B shows the stability of primary amines in the polymer film on porous HA disks in ambient air up to 65 days from the day of plasma polymerization. The

atomic percentage of the primary amine, $–NH_2$, represents the number of N atoms in the form of primary amine divided by the total number of all atoms, excluding hydrogen. It was observed that aging reduced the concentration of primary amines in the first month although this then became stable during the following month.

The chemical compositions at the 21 spots along the center axis on the cross section of porous HA disk, as shown in Fig. 1B, are presented in Fig. 3C. It was observed that, in the region very close to the top surface, the atomic percentage closely resembled that of the top surface and the C and N atomic percentages decreased along with the depth. The observed atomic percentages of N and O of 3-5 and 20-35 at.% indicated that plasma polymerization occurred even on the surfaces of the inner pores with a penetration depth of at least 2 mm.

SEM photos of outer surfaces of untreated and plasma treated porous HA are shown in Fig. 2D. Plasma polymerization did not cause structural changes of the porous disks. At x1000 magnification, interconnecting channels are clearly visible in both groups. The deposited polymer was not visible with SEM since its thickness was about 100 nm.

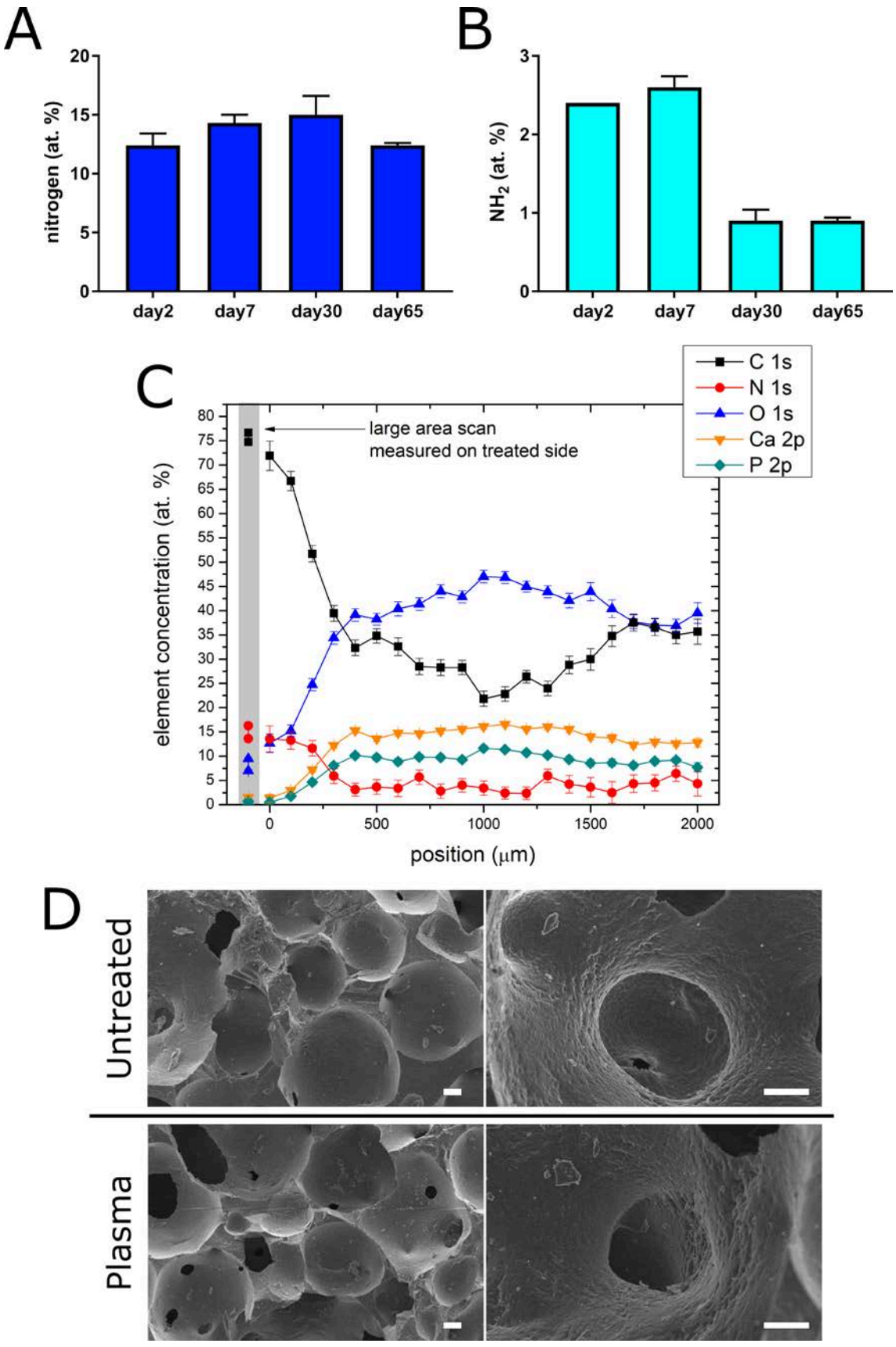
A
nitrogen (at. %)
20
15
10
5
0
day2
day7
day30
day65
B
NH2 (at. %)
3
2
1
0
day2
day7
day30
day65
C
C 1s
N 1s
O 1s
Ca 2p
P 2p
large area scan
measured on treated side
element concentration (at. %)
position (μm)
0
500
1000
1500
2000
D
Untreated
Plasma

Figure 2. Durability and penetration of plasma amine polymers. The atomic concentrations of nitrogen (A) and primary amines (B) were measured at day 2, 7, 30, and 65 following the CH_4/N_2/He plasma treatment. It was observed that the nitrogen content hardly changed over two months whereas the relative concentration of primary amines was reduced markedly during the first month. The profile of atomic concentrations along the center line of the CH_4/N_2/He plasma-treated disk is shown in (C). The cross-section geometry is given in Fig. 1B. It was observed that the polymer-depositing plasma penetrated from the top surface (i.e., position 0) into the inter-connected pores inside the disk up to the depth of 2 mm; i.e., the disk thickness. SEM photos of outer surfaces of untreated and plasma treated porous HA disks are shown in (D). Low magnification = x400. High magnification = x1000. Scale bars = 10 μm.

Effects of plasma treatment on cell behaviors

β-TCP are originally hydrophobic. CH_4/N_2/He plasma treatment in this study enhanced the hydrophilicity of the β-TCP (Supplementary Fig. S1A, B, Supplementary Movie S2) and cell adhesion to it.

Both cell counts and adhesion rate were all significantly higher on CH_4/N_2/He plasma-treated than the untreated β-TCP disks (Fig. 3A, 3B). The morphology of attached cells in the CH_4/N_2/He plasma-treated group following 24h incubation, presented a significant wider spreading cytoplasm (larger cell area) and showed a decreased circularity and solidity, which emphasized the presence of membrane protrusions (Fig. 3C, 3D)

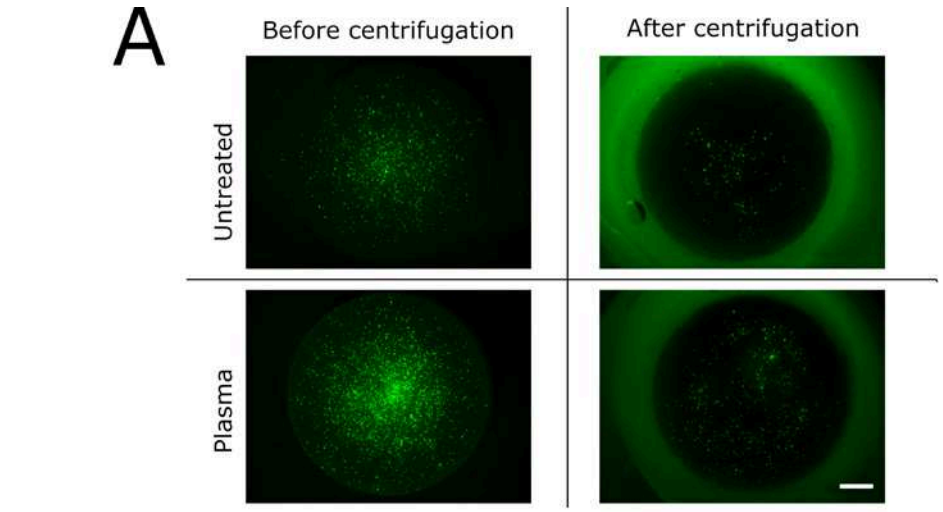
A
Before centrifugation
After centrifugation
Untreated
Plasma

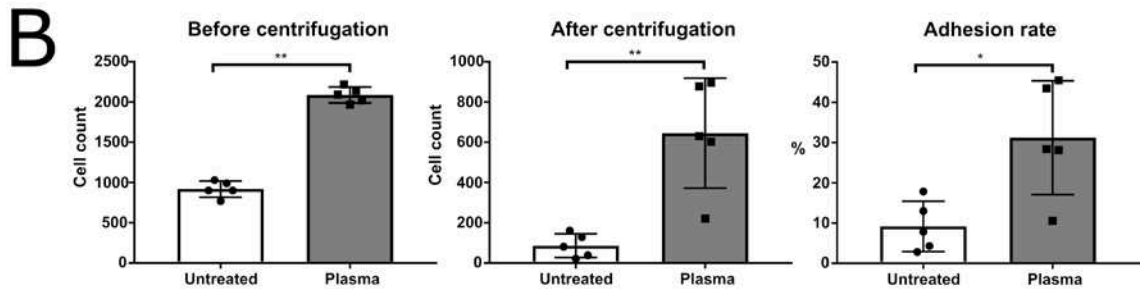
B
Before centrifugation
After centrifugation
Adhesion rate
Cell count
Cell count
%
Untreated
Plasma
Untreated
Plasma
Untreated
Plasma

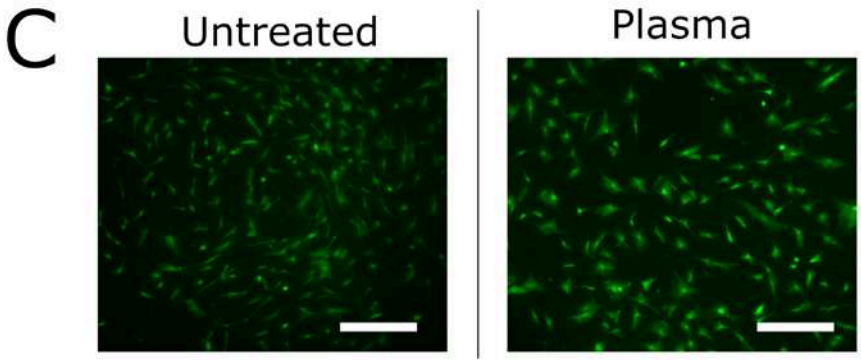
C
Untreated
Plasma

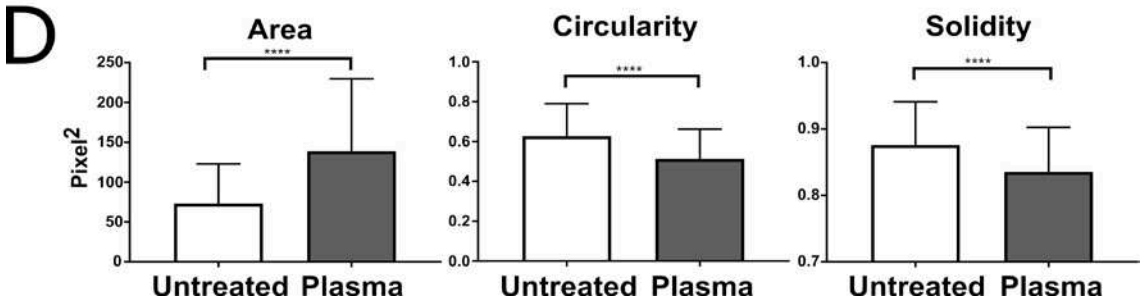
D
Area
Circularity
Solidity
Pixel2
Untreated
Plasma
Untreated
Plasma
Untreated
Plasma

Figure 3. Cell adhesion and morphology. (A) Fluorescence photos of BMSCs from GFP rats attached onto dense β-TCP disks before and after centrifugation. (B) Quantitative analysis of attached cells before and after centrifugation, and adhesion rate. Data are expressed as mean ± SD (n = 5). *p < 0.05, **p < 0.01. Mann-Whitney U test. (C) Fluorescence photos of attached cells on untreated or plasma-treated dense β-TCP disks. Scale bars = 500 μm. (D) Quantitative analysis of area, which represents the size, and solidity which represents the shape of attached cells. Data are expressed as mean ± SD with n = 1860 for “untreated” and n = 1440 for “plasma”. ****p < 0.0001. T-test.

CH_4/N_2/He plasma treatment did not significantly influence cell proliferation (Fig. 4A), but also significantly improved osteogenic differentiation as demonstrated by ALP staining (Fig. 4B, 4C) and ALP activity assay (Fig. 4D).

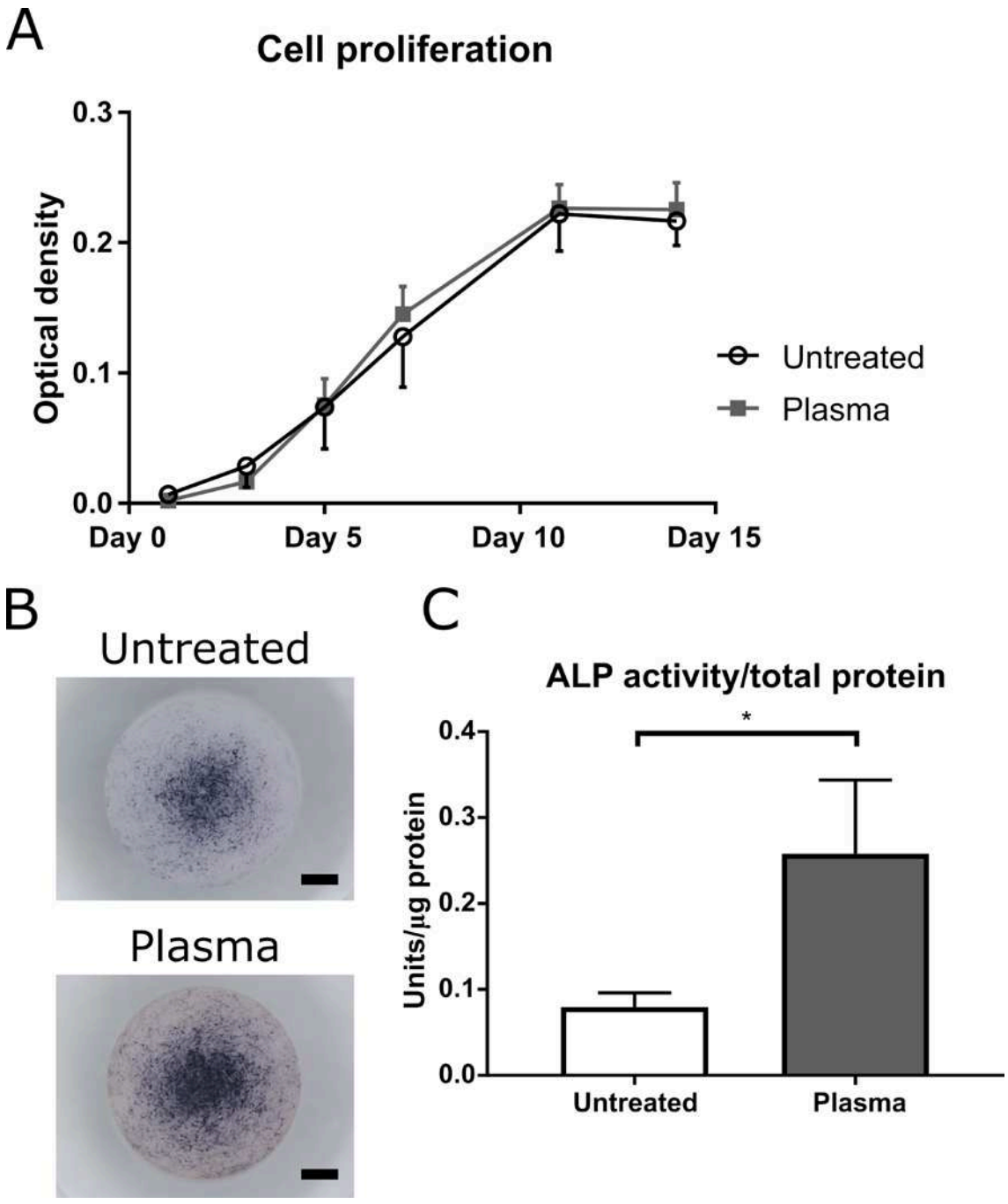

Figure 4. *In vitro* cell proliferation and osteogenic differentiation of GFP rat BMSCs. Cell proliferation curve (A). Macro photos of ALP-stained BMSCs from GFP rats sub-cultured on untreated (B) and $CH_4/N_2/He$ plasma-treated (C) dense β-TCP disks. Scale bars = 1 mm. ALP activity assay (D). ALP activity was normalized by total protein content. Data are expressed as mean ± SD (n = 3). *$p < 0.05$. T-test.

CH_4/N_2/He plasma treatment enhances new bone formation in vivo

Figure 5 shows micro-CT slices and corresponding histological sections (Fig. 5A, 5B: “Untreated”; 5E, 5F: “Plasma-treated”). Magnified histological images of the center and interface regions demonstrated more abundant bone formation and solid interface union in the CH_4/N_2/He plasma-treated (Fig. 5C, 5D) than in the untreated group (Fig. 5G, 5H) at postoperative 6 weeks.

At 3 weeks, volumes of new bones were observed inside the CH_4/N_2/He plasma-treated porous β-TCP disks and did not differ from the untreated porous β-TCP disks. At 6 weeks, the new bone inside the CH_4/N_2/He plasma-treated porous β-TCP disks was significantly higher than the untreated β-TCP disks (Fig. 5I). The 3D-reconstructed image of extracted new bone along with the host cranial bone revealed the abundant new bone formation in the CH_4/N_2/He plasma-treated β-TCP disk (Fig. 5J). In both groups, nearly one-third of the β-TCP was resorbed during 3 to 6 weeks (Fig. 5K) in similar resorption speed.

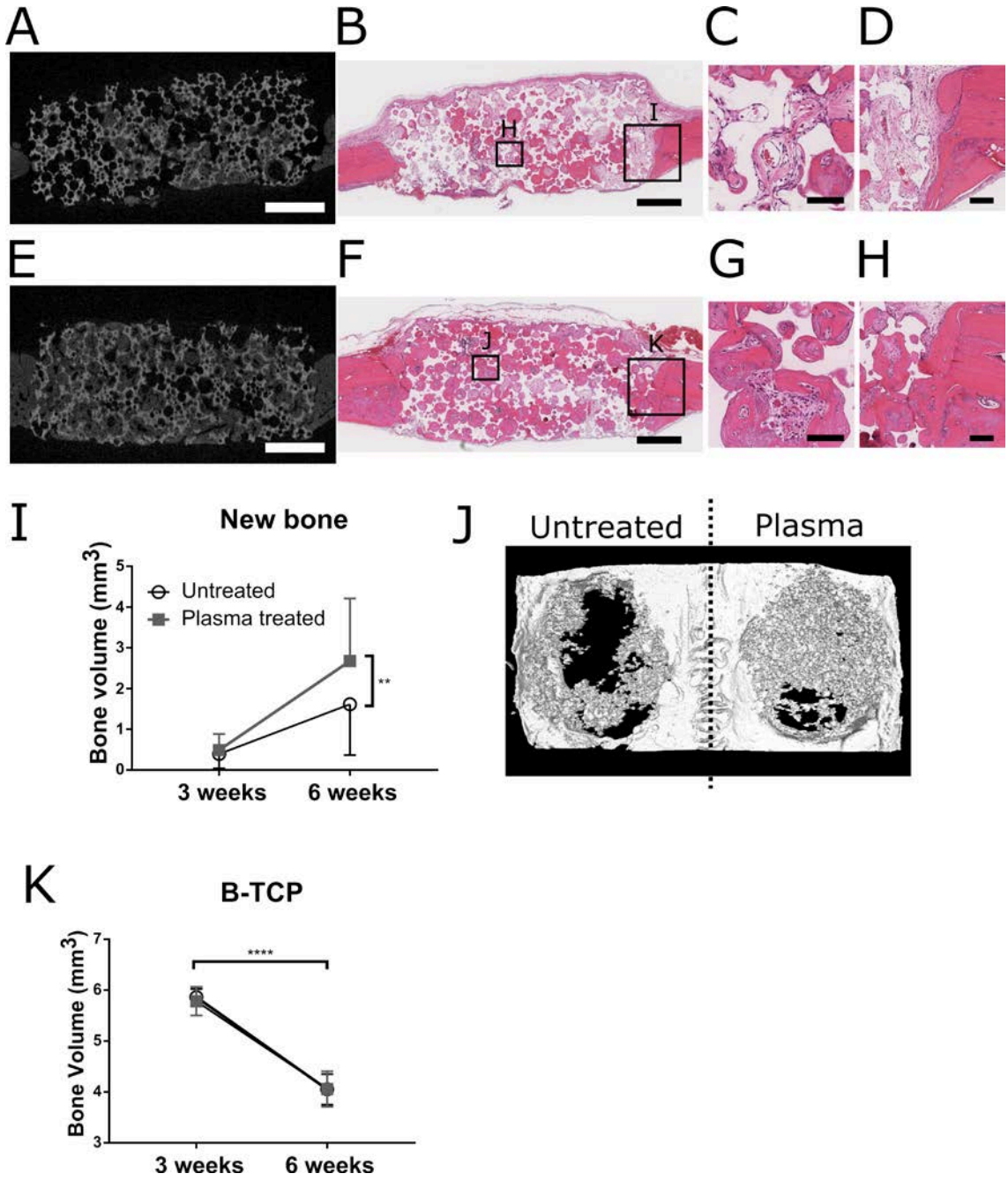

Figure 5. CH_4/N_2/He plasma treatment promotes bone formation inside β-TCP. Micro-CT slices and the corresponding histological sections stained with H&E of the untreated (A, B) and the plasma-treated group (E, F. Scale bars for D–G = 1 mm) at postoperative 6 weeks. Magnified images of the center and interface regions (C, D: "Untreated" group; G, H: "Plasma-treated" group. Scale bars = 100 μm). (I) Micro-CT

analysis of newly formed bone volumes between the plasma-treated and untreated group at 6 weeks. (J) 3D reconstruction of calvarial bone implanted with treated and untreated β-TCP (6 weeks, left: “Untreated”, right: “Plasma-treated”. Scale bar = 1 mm). Resorption rates of β-TCP between plasma-treated and untreated groups (K). Data are expressed as mean ± SD (n = 5 for 3 weeks, n = 15 for 6 weeks). **$p < 0.01$, ****$p < 0.0001$. Wilcoxon matched-pairs signed rank test.

Discussion

In this study, we generated a thin, stable amine-rich carbon polymer on the surface of calcium phosphates (HA and β-TCP) by low-pressure plasma technology using a mixed gas containing CH_4/N_2/He as precursors.

Low-pressure CH_4/N_2/He plasma allows chemically reactive gaseous species to penetrate into small pores of the porous HA and β-TCP disks during the plasma treatment and induces plasma polymerization on the inner surfaces of interconnected pores. In the present study, the top surface was completely covered with the amine-rich carbon polymers, and about 72–78% of the cross-section area distant from the top surface was covered with the amine-rich carbon polymers.

Through XPS measurements, we confirmed that under the same plasma conditions, plasma polymerization on the outer surface of both HA and β-TCP disks occurs in a similar manner regardless of disk type or composition. Therefore, extensive and systematic surface analyses of plasma-treated artificial bone were performed only with porous HA disks, with the expectation that the obtained results should also apply to plasma polymerization on β-TCP disks. Considering

the increasing use of β-TCP as the clinical product of bone substitute, cell and animal studies were performed with the CH_4/N_2/He plasma treated β-TCP disks. The results showed that CH_4/N_2/He plasma treatment had enhanced the hydrophilicity, *in vitro* cell migration, adhesion, osteogenic differentiation and *in vivo* bone regeneration of the β-TCP.

Stability of the amine-rich carbon polymer and its enhancement of osteogenic differentiation are considered to be the main mechanisms underlying this enhanced bone regeneration capacity.

As the surface N concentration did not substantially change over the first two months, the primary amines were considered to have been converted to secondary or ternary amines, mostly likely by oxidation. Notably, the reduction of primary amines in plasma polymers does not necessarily indicate the reduction of their biological effects as secondary or even ternary amines embedded in plasma polymers may have similar biological effects. However, determining how different amino groups interact within biological systems is beyond the scope of the current study.

Amine constitutes a hydrophilic functional group. The present study demonstrated that amine modification of calcium phosphates could enhance its hydrophilicity, and fasten the infiltration of cell suspension dropped on the calcium phosphate surface. Notably, the CH_4/N_2/He plasma-treated β-TCP resorbed tissue fluid and rapidly became wet, in contrast to non-treated β-TCP, which remained almost completely dry during the implantation (Supplementary Fig. S3). Moreover, histological sections at early phase (postoperative 3 weeks) revealed denser tissue formation in the CH_4/N_2/He plasma-treated disks. Taken together,

these findings suggest that the amine-rich carbon polymers can efficiently promote early tissue integration into the deep center of the disks, which makes preliminary preparations for later bone regeneration.

β-TCP coated with amine-rich carbon polymers enhanced *in vitro* osteoblastic differentiation and *in vivo* new bone formation. Several effects provided by amine modification must likely contributed to this enhanced bone formation.

Firstly, amine modification strengthens cell adhesion by enhancing integrin binding, which has been shown to be required for osteoblastic differentiation [18-20]. In detail, cell adhesion is mainly mediated by the binding of cellular integrins and adhesive proteins such as fibronectin in the extra-cellular matrix. Hydrophilic and positively charged amines can increase the density of fibronectin and change its conformation [21]. These changes in fibronectin strengthen the cell adhesion via integrin [22-23] and trigger rapid phosphorylation of focal adhesion-associated tyrosine kinase (FAK) [24], subsequently triggering ERK/MAPK signaling to upregulate Runt-related transcription factor 2 (Runx2), which is a master regulator of osteoblastic differentiation [25-31].

In addition, amine modification was found to modulate the cell morphology (e.g., larger cell area and decreased circularity and solidity), which has been shown to be relevant to the osteogenic differentiation of rat mesenchymal stem cells [32]. Moreover, human mesenchymal stem cells exhibiting a spreading rather than a round shape appear inclined toward an osteogenic lineage as well [33]. The underlying mechanism is considered to involve upregulation of Ras homolog family member A (RHOA), a transcription factor that regulates the actin cytoskeleton, along with increased osteogenesis [32-34].

Lastly, positively charged amines can also improve osteogenesis by affecting pH [35]. In an aqueous environment, amine is protonated and becomes positively charged ($–NH_3^+$), which can increase the interfacial pH. A high pH environment around implant materials has been reported to enhance osteoblastic differentiation [35-36].

In summary, our results support that amine modification of calcium phosphates with low-pressure CH_4/N_2/He plasma influences cell adhesion, cell spreading, and possibly the interfacial environment of calcium phosphates (here β-TCP). We consider that these factors in combination underlie the high ability of the modified β-TCP to improve bone regeneration.

There are limitations to this study. Firstly, the stability of the amine modification was observed for only two months, which should be elongated in future study for confirmation of longer off-the-shelf use. Secondly, we investigated the bone regeneration capacity only by the calvarial defect model. The calvaria has a rich blood supply and therefore is easy for bone regeneration. Further investigations of the bone regeneration effects in harsh environment such as malunions of fractures is needed. Thirdly, as the volume of newly formed bone inside the pores of the β-TCP disks was tiny, we could only evaluate the bone volume even with even a high-resolution micro-CT, but could not evaluate other bone parameters such as trabecular numbers and thicknesses. Finally, lacking biomechanical tests, we do not exactly know the real strength of the regenerated bone.

In treatment of large bone defects with artificial bone, the successful introduction of cells and blood vessels at a substantial distance from the host bone remains challenging [37-38]. To treat “critical size” bone defects, pre-loading of

bone or vascular-forming cells or vascular transplantation inside artificial bones has been attempted [39-42], which usually require long and costly pre-treatments. In the present study, we have reported a “chemical modification” approach as a next-generation surface treatment and processing strategy to form a stable amine-rich carbon polymer on the surfaces of calcium phosphates (representative material of artificial bone) to improve their bone regeneration ability in vitro and in vivo.

Author contributions

J. Kodama, A.H.H., S.H., and T. Kaito designed the study; A.H.H., T.I. S.S., and S.H. performed the material development and plasma polymerization; A.H.H., M.M., T.I., D.N., L.Z., and S.H. performed the surface analyses of materials. J. Kodama and T. Kaito performed the *in vitro* and *in vivo* experiments; Y.U., J. Kushioka, R.O., K.H., T. Kamatani, D.T., H.T., S.N., S.T., T.M., and Y.S. contributed to the data analysis and interpretation; J. Kodama, A.A.H., S.H., and T. Kaito wrote the manuscript.

Data availability

The datasets generated and/or analysed during the current study are available from the corresponding authors on reasonable request.

Acknowledgements

The authors thank Mr. Ryota Chijimatsu, Ms. Mari Shinkawa and Ms. Fumiko Hirayama for their great technical assistance.

Funding: This work was supported by Innovation Bridge Grant offered by Office for Industry-University Co-creation and University Advancement, Co-creation Bureau, Osaka University [Ja19990016]; the Matching Planner Program, the Regional Industry-Academia Value Program, both offered by Japan Science and Technology Agency (JST); Osaka University International Joint Research Promotion Programs (Type B); Japan Society of the Promotion of Science (JSPS) Grant-in-Aid for Scientific Research(S) [15H05736]; JSPS Core-to-Core Program [JPJSCCA2019002]; Research Grant of The Nakatomi Foundation; one of the authors (A. A. H) was also financially supported by Research and Innovation in Science and Technology Project (RISET-PRO), Ministry of Research, Technology, and Higher Education of Indonesia; two of the authors (M. M. and. L. Z.) were supported by the Czech Science Foundation [18-12774S], and the projects CEITEC 2020 [LQ1601] and CzechNanoLab [LM2018110] funded by the Ministry of Education, Youth and Sports of the Czech Republic (MEYS CR).

COI

Takashi Kaito has received research funding from Aimedic MMT. This company had no role in the study design, decision to publish, or preparation of the manuscript.

Joe Kodama, Anjar Anggraini Harumningtyas, Tomoko Ito, Miroslav Michlíček, Satoshi Sugimoto, Yuichiro Ukon, Junichi Kushioka, Rintaro Okada, Takashi Kamatani, Kunihiko Hashimoto, Daisuke Tateiwa, Hiroyuki Tsukazaki, Shinichi Nakagawa, Shota Takenaka, Takahiro Makino, Yusuke Sakai, David Nečas, Lenka Zajíčková and Satoshi Hamaguchi declare no potential conflict of interest

relevant to this article.

References

1. Buser, Z.; Brodke, D. S.; Youssef, J. A.; Meisel, H. J.; Myhre, S. L.; Hashimoto, R.; Park, J. B.; Tim Yoon, S.; Wang, J. C., Synthetic bone graft versus autograft or allograft for spinal fusion: a systematic review. *J Neurosurg Spine* **2016,** *25* (4), 509-516.

2. Yoshikawa, H.; Myoui, A., Bone tissue engineering with porous hydroxyapatite ceramics. *J Artif Organs* **2005,** *8* (3), 131-6.

3. Nedela, O.; Slepicka, P.; Svorcik, V., Surface Modification of Polymer Substrates for Biomedical Applications. *Materials (Basel)* **2017,** *10* (10).

4. Lee, D. S.; Moriguchi, Y.; Myoui, A.; Yoshikawa, H.; Hamaguchi, S., Efficient modification of the surface properties of interconnected porous hydroxyapatite by low-pressure low-frequency plasma treatment to promote its biological performance. *Journal of Physics D: Applied Physics* **2012,** *45* (372001).

5. Moriguchi, Y.; Lee, D. S.; Chijimatsu, R.; Thamina, K.; Masuda, K.; Itsuki, D.; Yoshikawa, H.; Hamaguchi, S.; Myoui, A., Impact of non-thermal plasma surface modification on porous calcium hydroxyapatite ceramics for bone regeneration. *PLoS One* **2018,** *13* (3), e0194303.

6. Intranuovo, F. e. a.; Gristina, R.; Fracassi, L.; Lacitignola, L.; Crovace, A.; Favia, P., Plasma Processing of Scaffolds for Tissue Engineering and Regenerative Medicine. . *Plasma Chemistry and Plasma Processing* **2016,** *36*, 269-280.

7. Mwale, F.; Rampersad, S.; Ruiz, J.-C.; Pierre-Luc Girard-Lauriault, P.-L.; Petit, A.; Antoniou, J.; Lerouge, S.; Wertheimer, M., Amine-Rich Cell-Culture Surfaces for Research in Orthopedic Medicine. . *Plasma Medicine* **2011,** *1*, 115-133.

8. Kaito, T.; Myoui, A.; Takaoka, K.; Saito, N.; Nishikawa, M.; Tamai, N.; Ohgushi, H.; Yoshikawa, H., Potentiation of the activity of bone morphogenetic protein-2 in bone regeneration by a PLA-PEG/hydroxyapatite composite. *Biomaterials* **2005,** *26* (1), 73-9.

9. Sugimoto, S.; Kiuchi, M.; Takechi, S.; Tanaka, K.; Goto, S., Inverter plasma discharge system. *Surface and Coatings Technology* **2001,** *136*, 65-68.

10. Takechi, S.; Sugimoto, S.; Kiuchi, M.; Tanaka, K.; Goto, S., Operational parameter effects on inverter plasma performance. *Surface and Coatings Technology* **2001,** *136*, 69-72.

11. Favia, P.; Stendardo, M. V.; d'Agostino, R., Selective grafting of amine groups on polyethylene by means of NH3−H2 RF glow discharges. *Plasmas and Polymers* **1996,** *1*, 91-112.

12. Council, N. R., Guide for the Care and Use of Laboratory Animals: Eighth Edition (The National Academies Press, 2011).

13. Maniatopoulos, C.; Sodek, J.; Melcher, A. H., Bone formation in vitro by stromal cells obtained from bone marrow of young adult rats. *Cell Tissue Res* **1988,** *254* (2), 317-30.

14. Carpenter, A. E.; Jones, T. R.; Lamprecht, M. R.; Clarke, C.; Kang, I. H.; Friman, O.; Guertin, D. A.; Chang, J. H.; Lindquist, R. A.; Moffat, J.; Golland, P.; Sabatini, D. M., CellProfiler: image analysis software for identifying and quantifying cell phenotypes. *Genome Biol* **2006,** *7* (10), R100.

15. Hart, L. M.; Lauer, J. C.; Selig, M.; Hanak, M.; Walters, B.; Rolauffs, B., Shaping the Cell and the Future: Recent Advancements in Biophysical Aspects Relevant to Regenerative Medicine. *Journal of Functional Morphology and Kinesiology* **2018,** *3*.

16. Reyes, C. D.; Garcia, A. J., A centrifugation cell adhesion assay for high-throughput screening of biomaterial surfaces. *J Biomed Mater Res A* **2003,** *67* (1), 328-33.

17. Schneider, C. A.; Rasband, W. S.; Eliceiri, K. W., NIH Image to ImageJ: 25 years of image analysis. *Nat Methods* **2012,** *9* (7), 671-5.

18. Keselowsky, B. G.; Collard, D. M.; Garcia, A. J., Integrin binding specificity regulates biomaterial surface chemistry effects on cell differentiation. *Proc Natl Acad Sci U S A* **2005,** *102* (17), 5953-7.

19. Lee, M. H.; Ducheyne, P.; Lynch, L.; Boettiger, D.; Composto, R. J., Effect of biomaterial surface properties on fibronectin-alpha5beta1 integrin interaction and cellular attachment. *Biomaterials* **2006,** *27* (9), 1907-16.

20. Moursi, A. M.; Globus, R. K.; Damsky, C. H., Interactions between integrin receptors and fibronectin are required for calvarial osteoblast differentiation in vitro. *J Cell Sci* **1997,** *110 (Pt 18)*, 2187-96.

21. Keselowsky, B. G.; Collard, D. M.; Garcia, A. J., Surface chemistry modulates fibronectin conformation and directs integrin binding and specificity to control cell adhesion. *J Biomed Mater Res A* **2003,** *66* (2), 247-59.

22. Keselowsky, B. G.; Collard, D. M.; Garcia, A. J., Surface chemistry modulates focal adhesion composition and signaling through changes in integrin binding. *Biomaterials* **2004,** *25* (28), 5947-54.

23. Michael, K. E.; Vernekar, V. N.; Keselowsky, B. G.; Meredith, J. C.; Latour, R. A.; García, A. J., Adsorption-Induced Conformational Changes in Fibronectin Due to Interactions with Well-Defined Surface Chemistries. *Langmuir* **2003,** *19*, 8033-8040.

24. Kornberg, L.; Earp, H. S.; Parsons, J. T.; Schaller, M.; Juliano, R. L., Cell adhesion or integrin clustering increases phosphorylation of a focal adhesion-associated tyrosine kinase. *J Biol Chem* **1992,** *267* (33), 23439-42.

25. Biggs, M. J.; Dalby, M. J., Focal adhesions in osteoneogenesis. *Proc Inst Mech Eng H* **2010,** *224* (12), 1441-53.

26. Biggs, M. J.; Richards, R. G.; Gadegaard, N.; Wilkinson, C. D.; Oreffo, R. O.; Dalby, M. J., The use of nanoscale topography to modulate the dynamics of adhesion formation in primary

osteoblasts and ERK/MAPK signalling in STRO-1+ enriched skeletal stem cells. *Biomaterials* **2009,** *30* (28), 5094-103.

27. Ge, C.; Xiao, G.; Jiang, D.; Franceschi, R. T., Critical role of the extracellular signal-regulated kinase-MAPK pathway in osteoblast differentiation and skeletal development. *J Cell Biol* **2007,** *176* (5), 709-18.

28. Hamilton, D. W.; Brunette, D. M., The effect of substratum topography on osteoblast adhesion mediated signal transduction and phosphorylation. *Biomaterials* **2007,** *28* (10), 1806-19.

29. Kanno, T.; Takahashi, T.; Tsujisawa, T.; Ariyoshi, W.; Nishihara, T., Mechanical stress-mediated Runx2 activation is dependent on Ras/ERK1/2 MAPK signaling in osteoblasts. *J Cell Biochem* **2007,** *101* (5), 1266-77.

30. Klees, R. F.; Salasznyk, R. M.; Kingsley, K.; Williams, W. A.; Boskey, A.; Plopper, G. E., Laminin-5 induces osteogenic gene expression in human mesenchymal stem cells through an ERK-dependent pathway. *Mol Biol Cell* **2005,** *16* (2), 881-90.

31. Liu, J.; Zhao, Z.; Li, J.; Zou, L.; Shuler, C.; Zou, Y.; Huang, X.; Li, M.; Wang, J., Hydrostatic pressures promote initial osteodifferentiation with ERK1/2 not p38 MAPK signaling involved. *J Cell Biochem* **2009,** *107* (2), 224-32.

32. Rocca, A.; Marino, A.; Rocca, V.; Moscato, S.; de Vito, G.; Piazza, V.; Mazzolai, B.; Mattoli, V.; Ngo-Anh, T. J.; Ciofani, G., Barium titanate nanoparticles and hypergravity stimulation improve differentiation of mesenchymal stem cells into osteoblasts. *Int J Nanomedicine* **2015,** *10*, 433-45.

33. McBeath, R.; Pirone, D. M.; Nelson, C. M.; Bhadriraju, K.; Chen, C. S., Cell shape, cytoskeletal tension, and RhoA regulate stem cell lineage commitment. *Dev Cell* **2004,** *6* (4), 483-95.

34. Bhadriraju, K.; Yang, M.; Alom Ruiz, S.; Pirone, D.; Tan, J.; Chen, C. S., Activation of ROCK by RhoA is regulated by cell adhesion, shape, and cytoskeletal tension. *Exp Cell Res* **2007,** *313* (16), 3616-23.

35. Shen, Y.; Liu, W.; Wen, C.; Pan, H.; Wang, T.; Darvell, B. W.; Lu, W. W.; Huang, W., Bone regeneration: Importance of local pH - Strontium-doped borosilicate scaffold. *J Mater Chem* **2012,** *22*, 8662-8670.

36. Shen, Y.; Liu, W.; Lin, K.; Pan, H.; Darvell, B. W.; Peng, S.; Wen, C.; Deng, L.; Lu, W. W.; Chang, J., Interfacial pH: a critical factor for osteoporotic bone regeneration. *Langmuir* **2011,** *27* (6), 2701-8.

37. Almubarak, S.; Nethercott, H.; Freeberg, M.; Beaudon, C.; Jha, A.; Jackson, W.; Marcucio, R.; Miclau, T.; Healy, K.; Bahney, C., Tissue engineering strategies for promoting vascularized bone regeneration. *Bone* **2016,** *83*, 197-209.

38. Mankin, H. J.; Gebhardt, M. C.; Jennings, L. C.; Springfield, D. S.; Tomford, W. W., Long-term results of allograft replacement in the management of bone tumors. *Clin Orthop Relat Res* **1996,** (324), 86-97.

39. Akita, S.; Tamai, N.; Myoui, A.; Nishikawa, M.; Kaito, T.; Takaoka, K.; Yoshikawa, H., Capillary vessel network integration by inserting a vascular pedicle enhances bone formation in tissue-engineered bone using interconnected porous hydroxyapatite ceramics. *Tissue Eng* **2004,** *10* (5-6), 789-95.

40. Deng, Y.; Jiang, C.; Li, C.; Li, T.; Peng, M.; Wang, J.; Dai, K., 3D printed scaffolds of calcium silicate-doped beta-TCP synergize with co-cultured endothelial and stromal cells to promote vascularization and bone formation. *Sci Rep* **2017,** *7* (1), 5588.

41. Nishikawa, M.; Myoui, A.; Ohgushi, H.; Ikeuchi, M.; Tamai, N.; Yoshikawa, H., Bone tissue engineering using novel interconnected porous hydroxyapatite ceramics combined with marrow mesenchymal cells: quantitative and three-dimensional image analysis. *Cell Transplant* **2004,** *13* (4), 367-76.

42. Zhang, D.; Gao, P.; Li, Q.; Li, J.; Li, X.; Liu, X.; Kang, Y.; Ren, L., Engineering biomimetic periosteum with beta-TCP scaffolds to promote bone formation in calvarial defects of rats. *Stem Cell Res Ther* **2017,** *8* (1), 134.

Figures

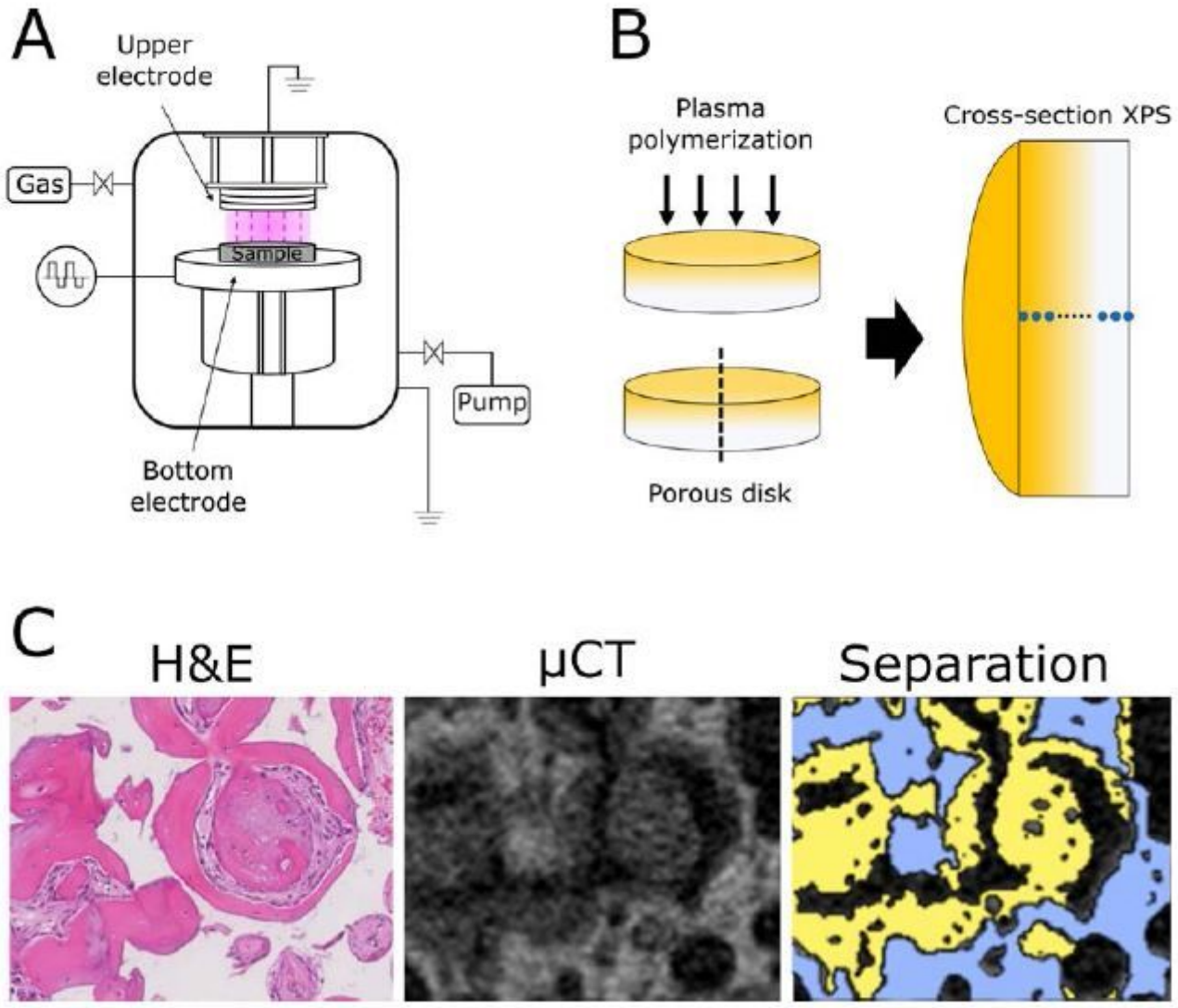

Figure 1

Plasma generation system, methodology of cross-section XPS analysis and micro CT evaluation. (A) Schematic diagram of the pulsed-plasma deposition system used in this study. Samples were placed on the bottom electrode. The discharge chamber was filled with a gas mixture of CH4, N2, and He at 70 Pa and bipolar high- voltage short pulses were applied to the bottom electrode periodically to generate the plasma. (B) Schematic diagram of cross-section XPS analysis. A porous disk was treated with the plasma on a single side and cut in half to expose the cross section. Then, the chemical compositions along the center axis were measured. (C) H&E-stained histological sections and corresponding micro-CT slices were compared to identify β-TCP (blue area) and newly formed bone (yellow area). Unstained areas in histological sections constitute the areas containing remaining β-TCP, which were decalcified. Pink areas stained by eosin reflect newly formed bone inside the β-TCP, which correspond to the gray areas in

micro-CT slices. An original algorithm was designed to extract and calculate the volume of β-TCP and newly formed bone separately.

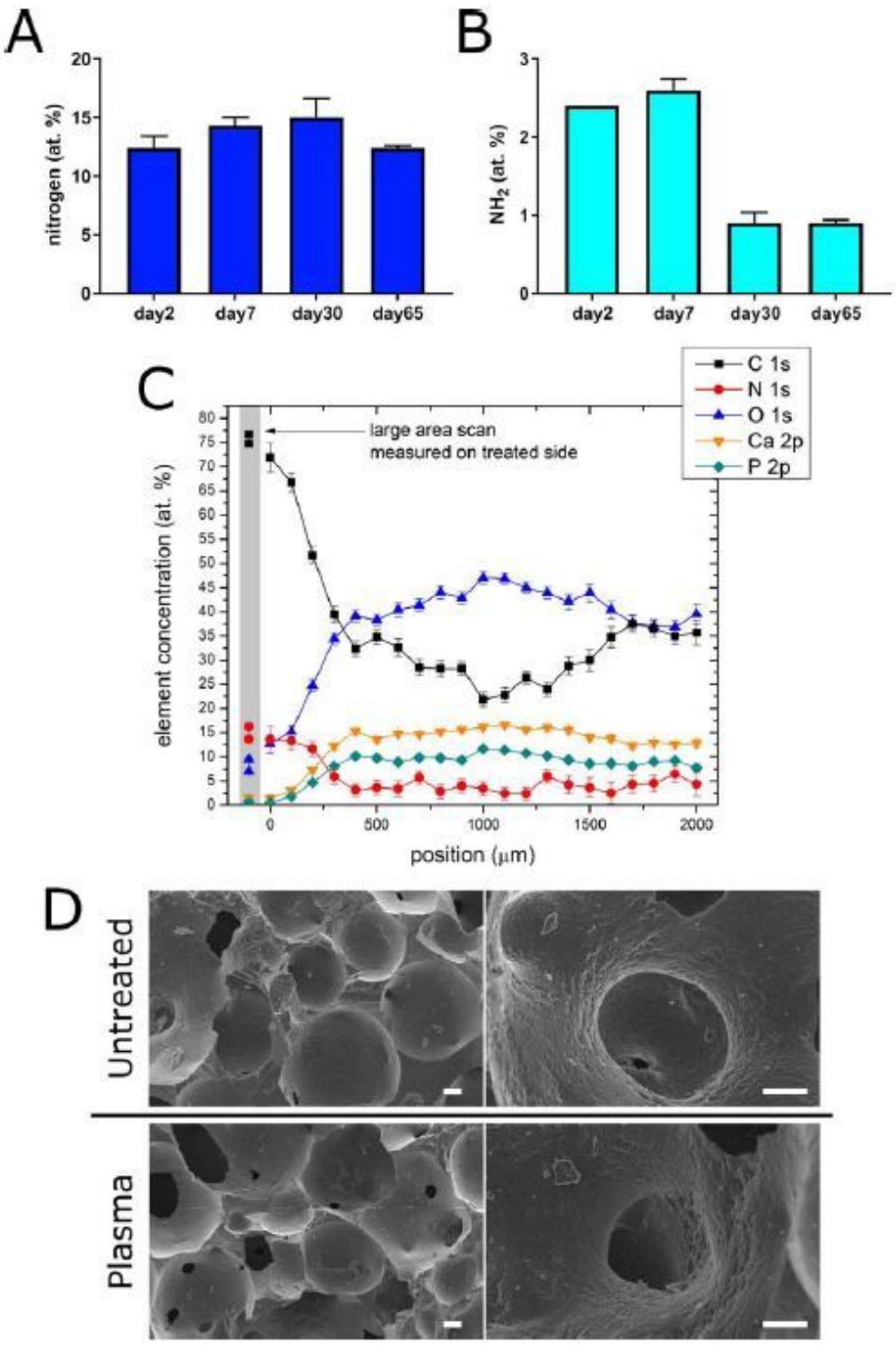

Figure 2

Durability and penetration of plasma amine polymers. The atomic concentrations of nitrogen (A) and primary amines (B) were measured at day 2, 7, 30, and 65 following the CH4/N2/He plasma treatment. It was observed that the nitrogen content hardly changed over two months whereas the relative

concentration of primary amines was reduced markedly during the first month. The profile of atomic concentrations along the center line of the CH4/N2/He plasma-treated disk is shown in (C). The cross-section geometry is given in Fig. 1B. It was observed that the polymer-depositing plasma penetrated from the top surface (i.e., position 0) into the inter-connected pores inside the disk up to the depth of 2 mm; i.e., the disk thickness. SEM photos of outer surfaces of untreated and plasma treated porous HA disks are shown in (D). Low magnification = x400. High magnification = x1000. Scale bars = 10 μm.

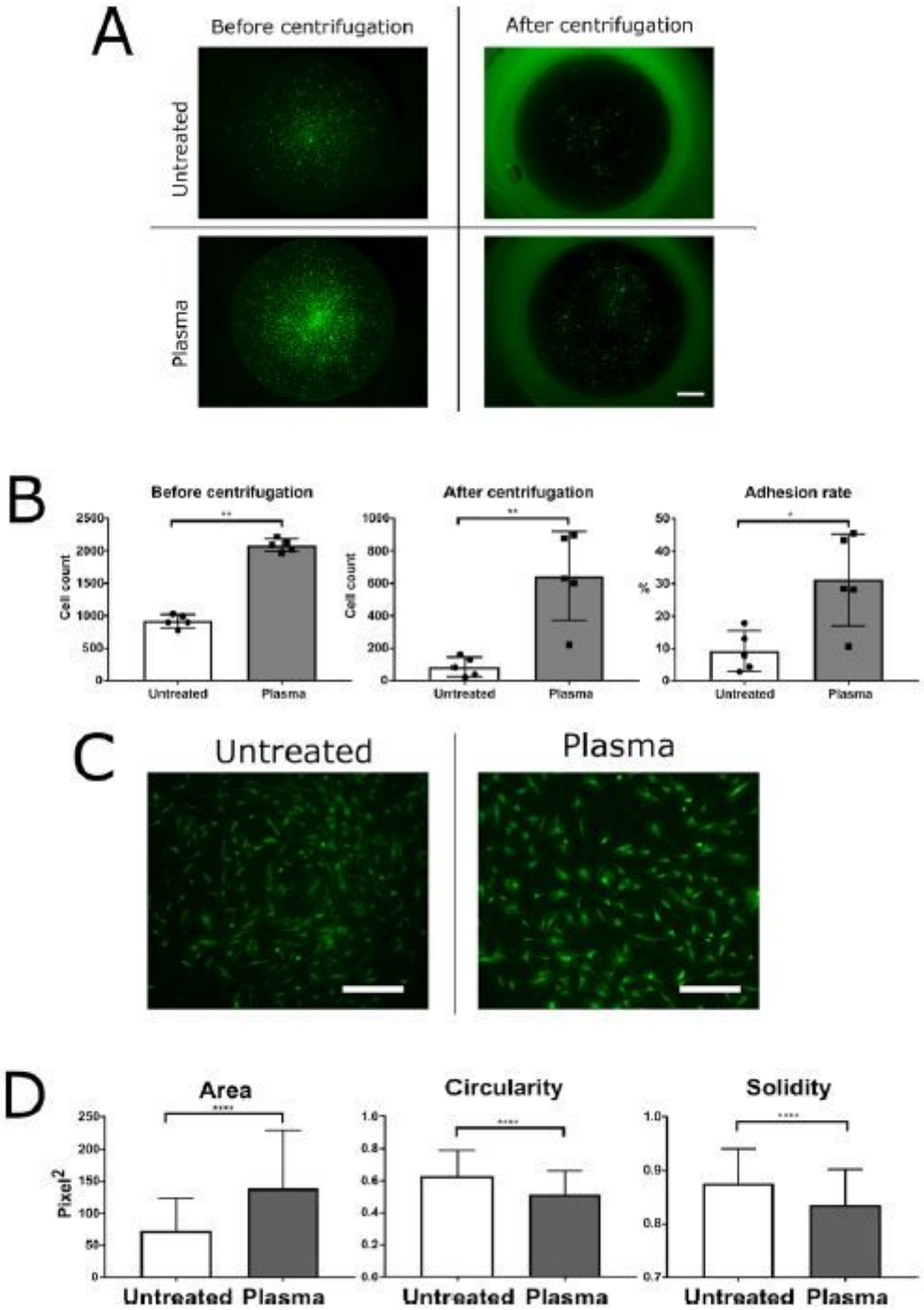

Figure 3

Cell adhesion and morphology. (A) Fluorescence photos of BMSCs from GFP rats attached onto dense β-TCP disks before and after centrifugation. (B) Quantitative analysis of attached cells before and after centrifugation, and adhesion rate. Data are expressed as mean ± SD (n = 5). *p < 0.05, **p < 0.01. Mann-Whitney U test. (C) Fluorescence photos of attached cells on untreated or plasma-treated dense β-TCP disks. Scale bars = 500 μm. (D) Quantitative analysis of area, which represents the size, and solidity which represents the shape of attached cells. Data are expressed as mean ± SD with n = 1860 for “untreated” and n = 1440 for “plasma”. ****p < 0.0001. T-test.

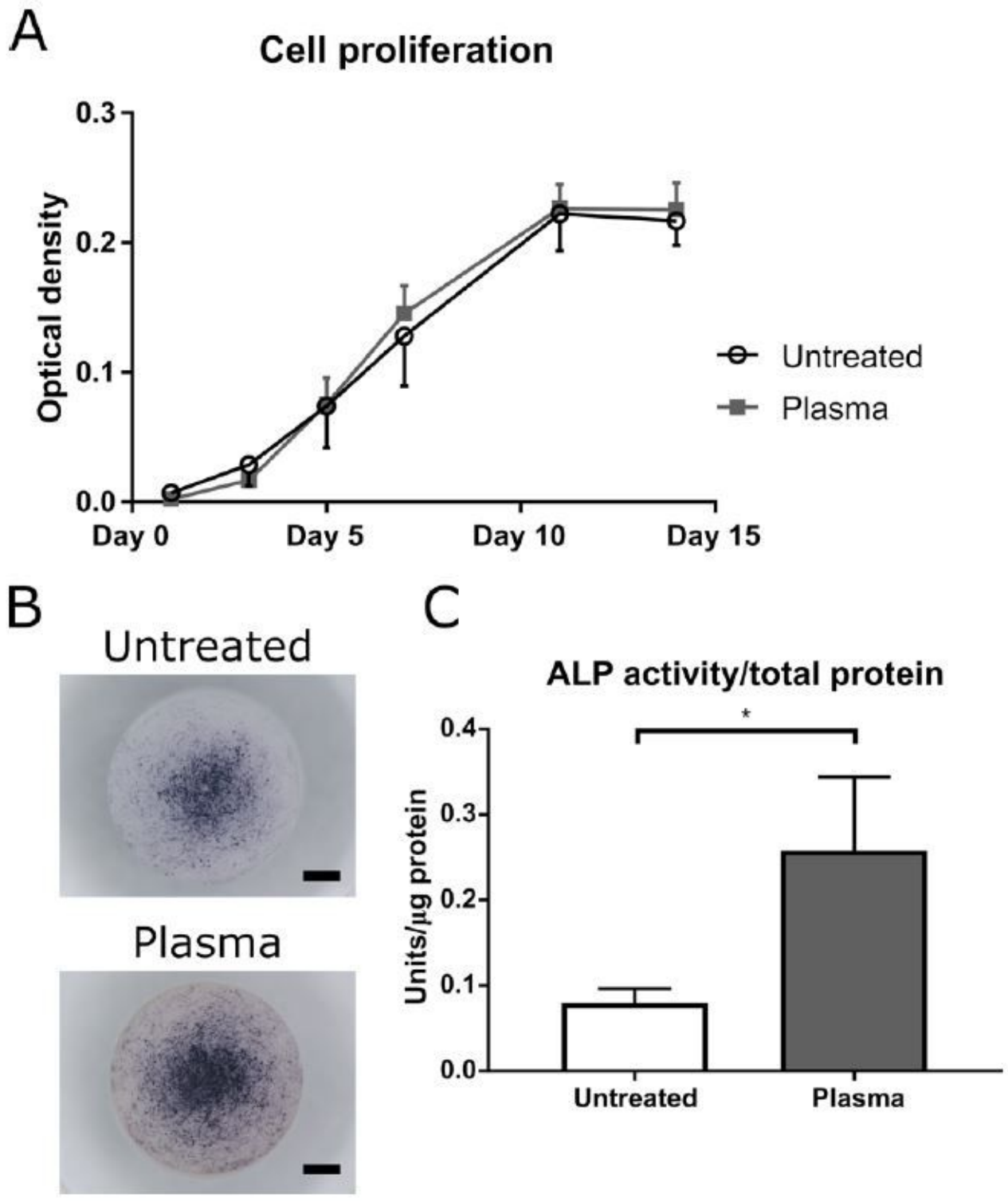

Figure 4

In vitro cell proliferation and osteogenic differentiation of GFP rat BMSCs. Cell proliferation curve (A). Macro photos of ALP-stained BMSCs from GFP rats sub-cultured on untreated (B) and CH4/N2/He plasma-treated (C) dense β-TCP disks. Scale bars = 1 mm. ALP activity assay (D). ALP activity was normalized by total protein content. Data are expressed as mean ± SD (n = 3). *p < 0.05. T-test.

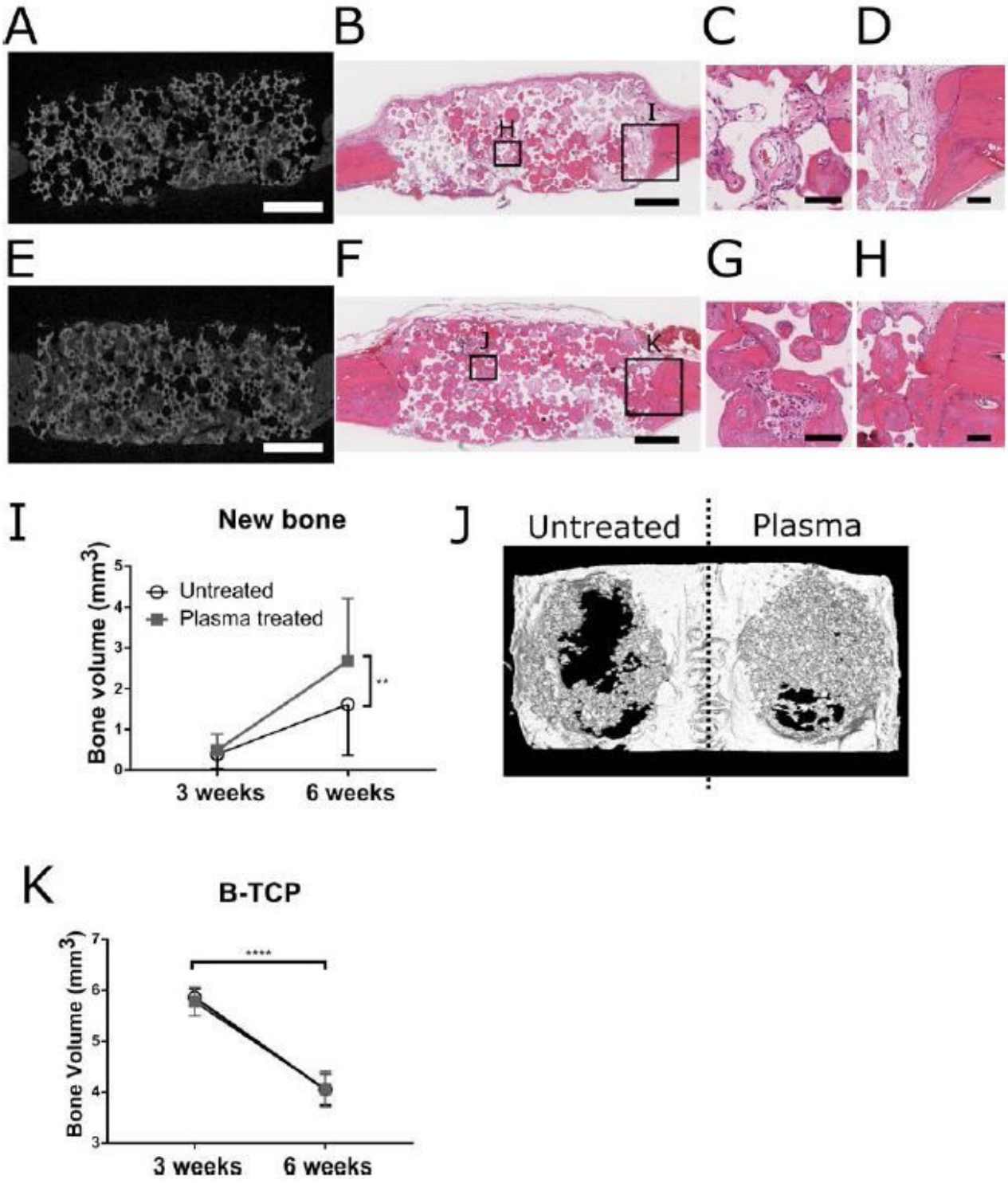

Figure 5

CH4/N2/He plasma treatment promotes bone formation inside β-TCP. Micro-CT slices and the corresponding histological sections stained with H&E of the untreated (A, B) and the plasma-treated group (E, F. Scale bars for D–G = 1 mm) at postoperative 6 weeks. Magnified images of the center and interface regions (C, D: “Untreated” group; G, H: “Plasma-treated” group. Scale bars = 100 μm). (I) Micro-CT analysis of newly formed bone volumes between the plasma-treated and untreated group at 6 weeks. (J) 3D reconstruction of calvarial bone implanted with treated and untreated β-TCP (6 weeks, left: “Untreated”, right: “Plasma-treated”. Scale bar = 1 mm). Resorption rates of β-TCP between plasma-treated and untreated groups (K). Data are expressed as mean ± SD (n = 5 for 3 weeks, n = 15 for 6 weeks). **p < 0.01, ****p < 0.0001. Wilcoxon matched-pairs signed rank test.

Supplementary Files

This is a list of supplementary files associated with this preprint. Click to download.

- Supplementaryinfo.pdf
- S2.mp4